



**HAL**  
open science

## Continuous circulation of an antigenically modified very virulent infectious bursal disease virus for fifteen years in Egypt

Ahmed Samy, Céline Courtillon, François-Xavier Briand, Mohamed Khalifa, Abdullah Selim, Abd El Satar Arafa, Ahmed Hegazy, Nicolas Eterradosi, Sébastien M. Soubies

### ► To cite this version:

Ahmed Samy, Céline Courtillon, François-Xavier Briand, Mohamed Khalifa, Abdullah Selim, et al.. Continuous circulation of an antigenically modified very virulent infectious bursal disease virus for fifteen years in Egypt. *Infection, Genetics and Evolution*, 2020, 78, pp.104099 -. 10.1016/j.meegid.2019.104099 . hal-03489086

HAL Id: hal-03489086

<https://hal.science/hal-03489086v1>

Submitted on 21 Jul 2022

**HAL** is a multi-disciplinary open access archive for the deposit and dissemination of scientific research documents, whether they are published or not. The documents may come from teaching and research institutions in France or abroad, or from public or private research centers.

L'archive ouverte pluridisciplinaire **HAL**, est destinée au dépôt et à la diffusion de documents scientifiques de niveau recherche, publiés ou non, émanant des établissements d'enseignement et de recherche français ou étrangers, des laboratoires publics ou privés.



Distributed under a Creative Commons Attribution - NonCommercial 4.0 International License

1 **Are wall thickness channels defined by computed tomography predictive of isthmuses of post-infarction**  
2 **ventricular tachycardia?**

3  
4  
5 Masateru Takigawa,MD<sup>\*1,2</sup>;Josselin Duchateau,MD<sup>\*1</sup>;Frederic Sacher,MD<sup>1</sup>;Ruairidh Martin,MD<sup>1,3</sup>;  
6 Konstantinos Vlachos,MD<sup>1</sup>;Takeshi Kitamura,MD<sup>1</sup>;Maxime Sermesant,PhD;Nicolas Cedilnik,PhD;Ghassen  
7 Cheniti,MD<sup>1</sup>;Antonio Frontera,MD<sup>1</sup>;Nathaniel Thompson,MD<sup>1</sup>;Calire Martin,MD<sup>1</sup>;Gregoire  
8 Massoullie,MD<sup>1</sup>;Felix Bourier,MD<sup>1</sup>;Anna Lam,MD<sup>1</sup>;Michael Wolf,MD<sup>1</sup>;William Escande,MD<sup>1</sup>;Clémentine  
9 André,MD<sup>1</sup>;Thomas Pambrun,MD<sup>1</sup>;Arnaud Denis,MD<sup>1</sup>;Nicolas Derval,MD<sup>1</sup>;Meleze Hocini,MD<sup>1</sup>;Michel  
10 Haissaguerre,MD<sup>1</sup>;Hubert Cochet,MD<sup>1</sup>;Pierre Jais,MD<sup>1</sup>

11  
12 Running Title: Relationship between CT-channel and VT-isthmus

13  
14 <sup>1</sup> Lyric institute, University of Bordeaux

15 <sup>2</sup>Heart Rhythm Center, Tokyo Medical and Dental university

16 <sup>3</sup>Institute of Genetic Medicine, Newcastle University, Newcastle-upon-Tyne

17 <sup>\*</sup>Both authors are equally contributed to the study.

18  
19 Address for correspondence: Masateru Takigawa

20 Service de Rythmologie,Hôpital Cardiologique du Haut Lévêque - (CHU) de Bordeaux,

21 Avenue de Magellan,33604 Bordeaux-Pessac,France.

22 Phone/FAX:+330556795679

23 E-mail:teru.takigawa@gmail.com

24

25 5000words; 4 Tables; 3 Figures

26

## 27 **DISCLOSURE**

28 Drs Haïssaguerre, Hocini, Jaïs and Sacher have received lecture fees from Biosense Webster and Abbott. Drs  
29 Denis, Derval, Jaïs and Sacher received speaking honoraria and consulting fees from Boston Scientific. Others  
30 have no conflict of interest to disclose.

31

## 32 **FUNDING**

33 Dr Martin: Fellowship (FS/16/71/32487) from the British Heart Foundation.

34 This work was supported by l'Agence Nationale de la Recherche [ANR-10-IAHU-04/ANR-11-EQPX-0030],  
35 and by the European Research Council [ERC n°715093]

36

37

## 38 **Abstract**

39

40 **Background:** Wall thickness in post-MI scar is heterogenous, with channels of relatively preserved thickness  
41 bordered by thinner scar.

42

43 **Objective:** This study sought to determine whether 3D-reconstructed CT-channels correlate with  
44 electrophysiological isthmuses during VT.

45

46 **Methods:** We retrospectively studied 9 post-infarction patients (age  $57\pm 15$  yrs, 1 female) with 10 complete  
47 VT activation maps (CL  $429\pm 77$ ms) created using an high-resolution mapping. 3D-reconstructed wall

48 thickness maps from CT were merged with the activation map during sinus rhythm (SR) and VT. The

49 relationship between WT and electrophysiological characteristics was analyzed.

50

51 **Results:** A total of 41 CT-channels were identified (median 4/pt), of median length 21.2mm (17.3-36.8mm),  
52 width 9.0mm(6.7-16.5mm), and area 1.49cm<sup>2</sup>(1.00-1.75cm<sup>2</sup>). WT in the channel was significantly thicker in  
53 the center than in the edge (median 2.4mm vs 1.5mm, P<0.0001). Of 3163 (2493-5960) mapping points in SR,  
54 382(191-1115) LAVAs were identified. One patient had a maximal proportion of LAVAs in 3-4mm, three  
55 patients in 2-3mm, two in 1-2mm, and two in 0-1mm. The VT-isthmuses of all 10 VTs corresponded with one  
56 to four CT-channels. Twenty one of the 41 CT-channels (51.2%) corresponded to a VT-isthmus (entrance,  
57 mid, or exit). Electrophysiological VT-isthmuses were more likely to be associated with CT-channels that  
58 were longer [P=0.04, OR 1.05/mm], thinner (but not less than 1mm) [P=0.03, OR 0.36/mm], or parallel to the  
59 mitral annulus [P=0.07, OR3.93].

60

61 **Conclusions:** VT-isthmuses were always found in CT-channels (100% sensitivity), and half of CT-channels  
62 hosted VT-isthmuses (PPV 51%). Longer and thinner (but >1mm) CT-channels were significantly associated  
63 with VT-isthmuses.

64

65 **Keywords;** ventricular tachycardia, contrast-enhanced multidetector computed tomography, high-resolution  
66 mapping, wall thickness, isthmus, myocardial infarction, MUSIC

67

68 **INTRODUCTION**

69

70 Visualization of potentially arrhythmogenic substrate obtained by cardiac imaging before and during an  
71 ablation procedure can help focus attention on culprit regions to treat ventricular tachycardia (VT).

72 Late gadolinium-enhanced cardiac magnetic resonance (CMR) is the reference technique for tissue  
73 characterization and spatial extent, topography, transmuralty and heterogeneity of myocardial scar.<sup>1,2</sup>

74 However, CMR-methods have substantial limitations in patients with VT in terms of availability,  
75 reproducibility across vendors/sites, quality and safety in patients with ICDs. Moreover, the spatial resolution

76 of conventional CMR-methods (usually several millimeters) may be inadequate to accurately characterize

77 severely remodeled chronic infarcts. In contrast, multi-detector computed tomography (MDCT) is more

78 readily available, highly reproducible across vendors/sites, less limited by ICDs, and has unparalleled spatial

79 resolution (about 500 $\mu$ m), and MDCT can accurately assess LV wall thickness (WT).<sup>5,6</sup> Wall thinning has

80 been shown to co-localize with voltage-defined scar (peak-to-peak bipolar amplitude < 1.5 mV)<sup>7</sup>, but to our

81 knowledge WT maps have not been directly compared to activation maps during VT. We hypothesized that

82 areas of severe thinning are indicative of denser scar acting as zones of conduction block, and that

83 VT-isthmuses would instead be observed in channels of relatively preserved thickness within scar. This study

84 aimed to characterize the relationship between WT channels derived from MDCT and VT-isthmuses as

85 defined by high density activation mapping.

86

## 87 **METHODS**

88

### 89 *Patient Selection*

90 Of 30 consecutive patients who underwent catheter ablation for post-myocardial infarction, VT using the  
91 Orion™ multipolar basket catheter and the Rhythmia™ system (Boston Scientific, Marlborough, MA, USA),  
92 9 patients with complete VT activation maps which covers an entire cycle length (CL) were included. All  
93 patients had episodes of repetitive, sustained VT requiring external cardioversion or ICD interventions. The  
94 research was approved by local ethics committees. Prior written informed consent to participate was obtained  
95 from all participants, according to institutional guidelines.

### 96 *Image Acquisition*

97 Contrast-enhanced MDCT was performed with a 2×192 detector dual-source scanner (Somatom Force,  
98 Siemens Healthcare, Forchheim, Germany), 1 to 3 days prior to the ablation procedure. Images were acquired  
99 in mid-diastole using prospective ECG-triggering during an expiratory breath-hold, with tube voltage and  
100 current adapted to patient morphology. Acquisition was performed in the arterial phase after the injection of a  
101 dual-phase bolus of iodinated contrast agent, i.e. 60mL of 100% contrast at the rate of 5 ml/s, followed by  
102 80mL of 50/50% contrast/saline at the same rate.

### 103 *Image Segmentation*

104 Image processing was performed by 2 trained technicians using the MUSIC platform (Liryc, Université de  
105 Bordeaux, Bordeaux & INRIA, Sophia Antipolis, France), as described previously<sup>8-11</sup>. Briefly, the cardiac  
106 chambers, ventricular epicardium, ascending aorta, and coronary sinus (CS) were segmented  
107 semi-automatically<sup>9</sup>, and ventricular endocardium automatically. WT was automatically computed from endo-  
108 and epicardial contours. We used 5-mm as a cutoff for significant myocardial thinning based on previously  
109 reported MDCT values of WT in a healthy population<sup>11</sup>. A 3-dimensional patient-specific model comprising  
110 all anatomical information was generated and exported in Matlab (The Mathworks, Inc., Nattick, MA) for  
111 subsequent post-hoc integration with electroanatomical geometries.

### 112 *Electrophysiological Study*

113 Electrophysiological studies were performed blinded from MDCT results. A 5-French decapolar and  
114 quadripolar catheter were placed in the CS and the right ventricle (RV), respectively. The LV endocardium  
115 was accessed using a transseptal approach. Pericardial access was obtained via a percutaneous subxiphoid  
116 puncture if required<sup>12,13</sup>. A voltage map was acquired with Rhythmia during both sinus rhythm (SR) and  
117 induced VT with the support of a steerable long sheath (Agilis, St Jude Medical, Saint-Paul, MN, USA).  
118 Activation maps were created using the standard beat acceptance criteria (automatic) based on (i) CL variation  
119 (ii) ECG QRS morphology, (iii) catheter motion (iv) electrogram stability (v) catheter tracking quality, and (vi)  
120 respiration gating. The confidence mask parameter was nominally set at 0.03mV, which was manually  
121 lowered to be as close as possible to the noise threshold, to allow visualization of the entire circuit.<sup>14,15</sup> In SR,  
122 all points within 2mm of the surface were analyzed, and local abnormal ventricular activities (LAVAs) were  
123 manually annotated in areas with coexisting LAVA and far-field activity. Areas of scar and dense scar were  
124 defined as <0.8 and <0.2 mV.<sup>16,17</sup> VT inducibility was assessed with 2 drive trains (600 and 400ms) with up to  
125 3 extrastimuli decremented to 200ms (or ventricular refractory period) from the RV apex after the creation of  
126 the activation map during SR. After the induction of VT, sustained VT was mapped and ablation was  
127 performed with the guidance of conventional activation and entrainment mapping. Regardless of VT  
128 termination with ablation, LAVA ablation was always subsequently performed with the endpoint of LAVA  
129 elimination.<sup>13</sup> Radiofrequency energy was delivered using an irrigated 3.5-mm-tip ablation catheter  
130 (Thermocool® SF catheter, Biosense Webster, Diamond Bar, CA), with a power of 35–50W endocardially  
131 and 25–35W epicardially. Where LAVA could be discerned to follow a distinct activation sequence on EAM,  
132 the earliest signals were targeted first. After ablation, the areas previously displaying LAVA were remapped.  
133 In the presence of residual LAVA, further radiofrequency ablation was performed. At the end of the procedure,  
134 induction of VT was repeated with programmed stimulation using the same protocol as before ablation.

### 135 *Post-hoc analysis*

136 The 3D- EAM was merged on the MDCT geometries on the Rhythmia™ system (Boston Scientific,  
137 Marlborough, MA) using identifiable anatomic reference points (Superior vena cava, inferior vena cava, left  
138 atrium, CS, aortic root, LV apex, and mitral annulus (MA) [3, 6, 9, and 12 o'clock]) to align both surfaces  
139 (Figure 1). The analyses were then performed using custom-built software in Matlab (The Mathworks, Inc.,

140 Nattick, MA). On MDCT data, a CT-channel was defined according to the following 3 criteria, as shown in  
141 Figure 2.

- 142 1. Abnormal thickness (<5 mm)
- 143 2. Thickness on both edges thinner than that inside the channel.
- 144 3. Length longer than width.

145 CT-channels were identified by a consensus of blinded analyses by 3 trained physicians (one radiologist and  
146 two electrophysiologists). The contours of each CT-channel were traced on the CT geometry.

147 On electroanatomical maps, a VT-isthmus was defined as follows.

- 148 1. Regions sequentially activated during the diastolic phase of VT
- 149 2. Confirmed by entrainment pacing<sup>18</sup> or direct termination during ablation on the site with the diastolic  
150 potentials.

151 Additionally, the VT-isthmus was divided into three portions based on the local activation time in the  
152 activation map in the present study; the first third of the diastolic phase is referred to as the entrance (early  
153 diastolic phase), the second third as the central isthmus (mid-diastolic phase), and the last third as the exit (late  
154 diastolic phase). Isthmuses and nearby edge zone areas were manually traced on the EAM geometry.

155 After registration, SR and VT maps, including electrophysiological isthmus segmentations, were projected on  
156 the CT geometry using a nearest-neighbor approach. This allowed automated comparison between  
157 electrophysiological findings and wall thickness measurements. Wall thickness and isthmus areas were  
158 directly compared with LAVA distributions. The spatial correlation between electrophysiological isthmuses  
159 and CT-channels was analyzed.

## 160 ***Statistical Analysis***

161 Categorical data were expressed as numbers and percentages. Continuous data for normally distributed  
162 variables were expressed as mean±SD and non-normally distributed data as median (25<sup>th</sup>-75<sup>th</sup> percentiles).

163 Comparisons were performed with, Student's t test or Kruskal-Wallis analysis. Logistic regression analysis



164 was performed to elucidate the factors predictive of CT-channels associated with VT-isthmuses. All tests were  
165 2-tailed, and a P value of <0.05 was considered statistically significant.

166

## 167 **RESULTS**

168

### 169 *Patient characteristics and characteristics of CT-channels*

170 The baseline characteristics of the 9 patients and CT-channel characteristics are shown in Table 1 and 2,  
171 respectively. Median thickness was 2.4[2.1-3.5] mm inside CT-channels, and 1.6[0.9-2.2] mm on their edges  
172 (P<0.0001). No channel was identified in regions thinner than 1mm and no edge region was identified in  
173 regions thicker than 4mm.

### 174 *VT Activation mapping and ablation*

175 The characteristics of VT activation maps are shown in Table 3. VT was induced in all patients. In total, 32  
176 different VTs (median 4 per patient) were observed, of which complete activation maps were acquired in 10  
177 (mean CL=429+/-77ms). In one patient (Pt-7), epicardial mapping was performed with a VT-isthmus, since  
178 neither diastolic potentials during VT nor LAVAs during SR were observed endocardially. Median length and  
179 width of VT-isthmuses measured on the 3D-EAM were 38+/-15mm. All VTs were terminated by ablation or  
180 mechanically terminated on the VT-isthmus except for one, which was overdrive-paced due to poor  
181 hemodynamic tolerance. Complete LAVA elimination was not achieved in 1/9 (11.1%) patient because of an

182 extensive LAVA distribution. Mean procedure and ablation times were  $280\pm 48$  min and  $57\pm 18$  minutes,  
183 respectively.

#### 184 *CT-thickness vs LAVA in SR*

185 All but one patients (incessant VT) had a voltage map during the sinus rhythm prior to VT induction and  
186 ablation. In a total of 35217 points, 1070(3.0%), 4164(11.8%), 4615(13.1%), 4277(12.1%), 3173(9.0%), and  
187 17918(50.9%) points were distributed in WT:0-1mm, WT:1-2mm, WT:2-3mm, WT:3-4mm, WT:4-5mm area,  
188 and normal thickness (WT>5mm) area, respectively; out of these points, 336 (31.6%), 1113 (26.7%), 1358  
189 (29.4%), 957 (22.4%), 475 (15.0%), and 922 (5.1%) showed LAVA potentials, respectively. One patient had a  
190 maximal proportion of LAVAs in 3-4mm, three patients in 2-3mm, two in 1-2mm, and two in 0-1mm.

#### 191 *CT-thickness channels vs. VT-isthmuses*

192 Of the 10 VTs in which the VT circuit was fully characterized by activation mapping covering an entire CL,  
193 all VT-isthmuses co-localized with CT-channels. Out of the 41 CT-channels identified in the population,  
194 21(51.2%) contained diastolic potentials during VT, including 13(31.7%) with mid-diastolic potentials. These  
195 electrical VT-isthmuses went through a single CT-channel in 3(30%) VTs, 2 CT-channels in 2(20%), 3  
196 CT-channels in 3(30.0%), and 4 CT-channels in 2(20.0%) (Supplemental table 1). Therefore, channels defined  
197 by CT predict involvement in a critical part of the VT circuit with a sensitivity of 100% and a positive  
198 predictive value of 51.2% (Supplemental table 2).

199 WT at the center of CT-channels was always above 1mm (Supplemental Figure 1A). WT on CT-channel  
200 edges was always less than 4mm (Supplemental Figure 1B). Examples of CT-channels containing diastolic

201 activity during VT are shown in Figure 3A/Video 1 and Figure 3B/Video 2. Table 4 compares the CT-channel  
202 characteristics between those hosting diastolic activation during VT and those that did not. Univariate analysis  
203 identified three significant morphological predictors of diastolic activation during VT, two of which remained  
204 independent predictors on the multivariate analysis: longer CT-channels (P=0.04, OR 1.05(1.00-1.10)),  
205 thinner (but>1mm) CT-channels (P=0.03, OR 0.36(0.14-0.90)). CT-channels parallel to the MA was weakly  
206 associated (P=0.07, OR 3.93(0.89-17.42)). A WT at CT-channel center of 1-4mm and a length >2cm  
207 predicted an electrophysiological VT-isthmus with 86% sensitivity and 60% specificity. CT-channels  
208 implicated in VT also had a higher proportion of LAVA, although the difference did not reach statistical  
209 significance (P=0.09).

#### 210 *Outcome during follow-up*

211 During a mean follow-up of 19.7±15.5 months, 2 patients had VT recurrence (Pt-3 and Pt-6). In the Pt-3, the  
212 index procedure failed to achieve complete LAVA elimination and a post-hoc analysis of CT-channel vs  
213 VT-isthmus showed that some of the CT-channels had not been completely transected. During the redo  
214 procedure, a VT with a different morphology from the index procedure was successfully mapped and  
215 terminated at a site with a mid-diastolic potential corresponding with one of the CT-channels, although using a  
216 different exit from the index VT. In the Pt-6, the index procedure ended with a complete LAVA elimination.  
217 The post-hoc analysis of CT-channel vs VT-isthmus showed that all regions matched to CT-channels were  
218 well ablated. As endocardial LAVAs were completely ablated in the index procedure, an epicardial approach  
219 was prepared for the redo procedure. The redo procedure identified 2VTs with different morphologies from

220 those observed during the index procedure, one of which was mappable. The epicardial map demonstrated  
221 mid-diastolic potentials at a site immediately opposite to the CT-channel identified on the endocardium and  
222 the VT was terminated at this site. Residual epicardial LAVAs identified in this area were all eliminated and  
223 no endocardial ablation was required. No recurrence was seen afterward in these two patients.

224

## 225 **DISCUSSION**

226

227 This study is, to our knowledge, the first to compare the distribution of CT-defined anatomical channels with  
228 VT-isthmuses. The main findings are that (1) CT wall thickness maps of the MI scar are feasible and identify  
229 CT-channels; (2) These CT-channels are thin, with edges thinner by at least 1 mm; (3) Electrical  
230 VT-isthmuses co-localize with one or more of the CT-channels in 100%, and 50% of CT-channels correspond  
231 to VT-isthmuses; (4) The CT-channels hosting VT-isthmuses may have some morphological characteristics.

### 232 ***CT-channel vs. VT-isthmus***

233 In the present study, we found that all VT-isthmuses used one or two CT-channels and that 51.2% of  
234 CT-defined channels hosted a VT-isthmus, (Sensitivity of 100% and positive predictive value of 51.2%)  
235 (Supplemental table 2).

236 Previous reports have shown that the scar extent on LGE-CMR is significantly associated with  
237 VT-inducibility and prognosis in patients with structural heart disease<sup>19,20</sup>. In addition, scar transmuralty,  
238 defined as the ratio of post-infarct scar thickness to left ventricular WT has been associated with EGM

239 characteristics on EAM<sup>1-3,21-22</sup>. The utility of both MDCT and CMR in VT ablation has been previously  
240 reported<sup>7,23</sup>, and MDCT has been shown to reliably identify areas of low voltage, identified using a 3D  
241 mapping system<sup>7,23</sup>. The present study provides the further possibility that CT-WT channels can be used to  
242 identify the VT-isthmus with high sensitivity. In post-MI scar, the thinnest parts (channel edges) are likely to  
243 have no or very few surviving bundles. They could therefore act as zones of block, or pseudo-block due to  
244 relatively slower transverse conduction, whereas the relatively thicker channels between the thinnest areas  
245 may host residual slowly conducting bundles.

246 Although MDCT may identify VT isthmuses, it does not identify whether the channel should be approached  
247 from the endocardium versus the epicardium. In Pt-6, all the pre-procedure CT channels appeared to have  
248 been ablated using the conventional approach, yet the patient had VT recurrence requiring an epicardial  
249 approach. Further, in Pt-7, VT with an epicardial isthmus was observed even though no LAVAs were  
250 identified endocardially. Although the endocardial approach is usually sufficient post myocardial infarction,  
251 an epicardial approach may be also taken into consideration for re-do procedures where transection of all  
252 channels was achieved in the index procedure.

### 253 *CT-channel characteristics more associated with mapped VT-isthmuses*

254 As some rapid or unstable VTs were not successfully mapped, we were unable to demonstrate a relationship  
255 between the VT-isthmuses and CT-channels in these VTs. Nevertheless, some morphological characteristics  
256 were statistically associated with mapped VT-isthmuses. Thinner, longer channels, and channels parallel to  
257 the MA were more frequently functional (associated with a mapped VT-isthmus). However, even long

258 CT-channels are not systematically predictive of VT-isthmuses, particularly in thicker tissue. This observation  
259 fits well with another observation in our study, that LAVAs are much less frequent when wall thickness is  
260 above 4mm. In these regions, myocardium is healthier, most likely associated with more normal conduction  
261 properties, and therefore less likely to participate in a VT-isthmus. These morphological characteristics may  
262 be useful to guide ablation of the higher-risk CT-channels. However, more data should be collected; although  
263 the channel morphologies were different between those supporting VT and those not, there was significant  
264 overlap between groups. Further, the association between VT-isthmuses and channels parallel to the MA  
265 further corroboration due to the weak statistical significance and lack of a theoretical explanation for the  
266 finding. Although one could speculate that channels bordered by basal scar and the MA support VT more  
267 frequently because the MA is a complete anatomical insulator. This is of major importance as we cannot rule  
268 out that some CT-channels are functional VT-isthmuses for VTs that were simply not induced in this study. A  
269 practical approach (aiming at the best single procedure success rate) could target all CT-channels in order to  
270 ensure the most comprehensive ablation of the VT substrate.

#### 271 *Relationship between wall thickness and LAVAs*

272 The present study also describes the distribution of LAVAs in the scar area using an high-resolution mapping  
273 system. 20-30% of all points in the  $WT \leq 4$  mm had LAVAs. Indeed, LAVAs were overall most frequently  
274 identified in the thinnest WT area (0-1mm). However, individually, LAVA distribution was highest in this  
275 thinnest area only in 2 patients, and CT-channels used as VT-isthmus were never found in these thinnest  
276 regions. These results suggest that LAVA distribution in the thinnest areas (<1mm) may be not associated

277 with the maintenance of VT despite the high prevalence of LAVAs. Although complete LAVA elimination is  
278 associated with better outcomes<sup>12</sup>, LAVA elimination in the thinnest areas may not be always necessary to  
279 avoid VT recurrence (at least in slow VT mapped in the present study). Although more detailed characteristics  
280 of LAVA such as voltage and/or delay may be associated with the maintenance of VT, LAVA distribution in  
281 SR itself may be not enough to narrow the ablation target.

### 282 *Clinical implications*

283 CT scans are easy to obtain, reproducible from center to center, and of very consistent quality, allowing for  
284 high spatial resolution assessment of the post MI Scar. Wall thickness maps describe CT-channels that host  
285 100% of VT-isthmuses. This information - available before the procedure - refines the substrate definition, is  
286 highly sensitive and could be more specific than the 3D-EAM of the substrate. By providing more specific  
287 and clearly defined ablation targets, this pre-procedural diagnostic phase could help the operator to use a more  
288 focused ablation strategy and shorten traditionally long VT ablation procedures.

### 289 *Study limitations*

290 The first limitation of the present study is that not all VTs were mappable, and therefore the VTs mapped may  
291 not be representative of the whole population of VTs. VTs were not always sufficiently stable or tolerable for  
292 complete mapping. However, sufficient mapping data was acquired per patient and CT channel to allow for  
293 valid statistical analyses. Another limitation is related to the potential mis-registration between imaging and  
294 electroanatomical mapping geometries. This aspect was partly addressed by using state-of-the-art technologies  
295 embedded in 3D-EAM, and did not prevent identification of matching CT-channels and VT-isthmuses.

296 However, the geographical compatibility between the CT-image and 3D-EAM should be prospectively  
297 examined. Third, although the concept is likely to be similar in faster or unstable VTs, this is not proven as the  
298 findings are derived from stable slower VTs. Also, the applicability to non-ischemic VTs requires further  
299 assessment as the mechanism and distribution of scars (substrates) are different Fourth, especially in patients  
300 with ICD storm or incessant VTs, renal dysfunction may prevent contrast CT acquisition and therefore may  
301 limit generalizability of these results to sicker patients with VT. Finally, the efficacy and safety should be  
302 compared with a standard ablation strategy.

303

## 304 **CONCLUSION**

305

306 CT scan wall thickness maps identify CT-channels which host VT-isthmuses consistently. Half of the  
307 CT-defined channels are associated with the critical isthmus of mapped VT. If not all CT-channels are  
308 functional VT-isthmuses, perhaps due to VT non-inducibility, longer and thinner (but > 1mm) CT-channels  
309 parallel to the mitral annulus are more frequently associated with VT-isthmuses. The integration of these 3D  
310 models describing clear and focused targets could help to shorten VT ablation procedures, and potentially  
311 improve outcomes, but the clinical impact of this approach needs to be tested in further prospective trials.

312



## 313 **REFERENCES**

314

315 1. Desjardins B, Crawford T, Good E, et al. Infarct architecture and characteristics on delayed enhanced



- 316 magnetic resonance imaging and electroanatomic mapping in patients with postinfarction ventricular  
317 arrhythmia. *Heart Rhythm*.2009;6:644–651.
- 318 2. Wijnmaalen AP, van der Geest RJ, van Huls van Taxis CF et al. Head-to-head comparison of  
319 contrast-enhanced magnetic resonance imaging and electroanatomical voltage mapping to assess  
320 post-infarct scar characteristics in patients with ventricular tachycardias: real-time image integration and  
321 reversed registration. *Eur Heart J*.2011;32:104–114.
- 322 3. Dickfeld T,Tian J,Ahmad G,et al. MRI-guided ventricular tachycardia ablation: integration of late  
323 gadolinium-enhanced 3D scar in patients with implantable cardioverter-defibrillators. *Circ Arrhythm*  
324 *Electrophysiol*.2011;4:172–84.
- 325 4. Mesubi O, Ahmad G, Jeudy J, et al. Impact of ICD artifact burden on late gadolinium enhancement  
326 cardiac MR imaging in patients undergoing ventricular tachycardia ablation. *Pacing Clin Electrophysiol*.  
327 2014;37:1274–83.
- 328 5. Gerber BL, Belge B, Legros GJ, et al. Characterization of acute and chronic myocardial infarcts by  
329 multidetector computed tomography: comparison with contrast-enhanced magnetic resonance. *Circulation*.  
330 2006;113:823–833.
- 331 6. Kanza RE,Higashino H,Kido T, et al. Quantitative assessment of regional left ventricular wall thinning  
332 and thickening using 16 multidetector row computed tomography: comparison with cine magnetic  
333 resonance imaging. *Radiat Med*.2007;25:119–126.
- 334 7. Tian J,Jeudy J,Smith MF,et al. Three-dimensional contrast-enhanced multidetector CT for anatomic,  
335 dynamic, and perfusion characterization of abnormal myocardium to guide ventricular tachycardia  
336 ablations. *Circ Arrhythm Electrophysiol*.2010;3:496–504.
- 337 8. Komatsu Y, Cochet H, Jadidi A, et al. Regional myocardial wall thinning at multidetector computed  
338 tomography correlates to arrhythmogenic substrate in postinfarction ventricular tachycardia: Assessment

- 339 of structural and electrical substrate. *Circ Arrhythm Electrophysiol.* 2013;6:342-350. 
- 340 9. Cochet H, Komatsu Y, Sacher F, et al. Integration of merged delayed-enhanced magnetic resonance  
341 imaging and multidetector computed tomography for the guidance of ventricular tachycardia ablation: A  
342 pilot study. *J Cardiovasc Electrophysiol.* 2013;24:419-426. 
- 343 10. Yamashita S, Sacher F, Mahida S, et al. The role of high-resolution image integration to visualize left  
344 phrenic nerve and coronary arteries during epicardial ventricular tachycardia ablation. *Circ Arrhythm*  
345 *Electrophysiol.* 2015;8:371-380.
- 346 11. Stolzmann P, Scheffel H, Leschka S, et al. Reference values for quantitative left ventricular and left atrial  
347 measurements in cardiac computed tomography. *Eur Radiol.* 2008;18:1625–1634.
- 348 12. Sosa E, Scanavacca M, d'Avila A, Pilleggi F. A new technique to perform epicardial mapping in the  
349 electrophysiology laboratory. *J Cardiovasc Electrophysiol.* 1996;7:531–536.
- 350 13. Jaïs P, Maury P, Khairy P, et al. Elimination of local abnormal ventricular activities: a new end point for  
351 substrate modification in patients with scar-related ventricular tachycardia. *Circulation.* 2012;125:2184–  
352 2196.
- 353 14. Takigawa M, Derval N, Frontera A, et al. Revisiting anatomic macroreentrant tachycardia after atrial  
354 fibrillation ablation using ultrahigh-resolution mapping: Implications for ablation. *Heart*  
355 *Rhythm.* 2018;15:326-333
- 356 15. Takigawa M, Derval N, Martin CA, et al. A simple mechanism underlying the behavior of reentrant atrial  
357 tachycardia during ablation. *Heart Rhythm.* 2019;16:553-561.
- 358 16. Sacher F, Duchateau J, Capellino S, et al. Voltage threshold for high density mapping catheter with short  
359 interspaced small electrodes. *Heart Rhythm* 2016;13:S32. AB014–02.
- 360 17. Martin CA, Takigawa M, Martin R, et al. Use of Novel Electrogram "Lumipoint" Algorithm to Detect  
361 Critical Isthmus and Abnormal Potentials for Ablation in Ventricular Tachycardia. *JACC Clin*  
362 *Electrophysiol.* 2019;5:470-479.
- 363 18. Stevenson WG, Friedman PL, Sager PT, et al. Exploring postinfarction reentrant ventricular tachycardia

- 364 with entrainment mapping. *J Am Coll Cardiol.*1997;29:1180-1189.
- 365 19. Roes SD,Borleffs CJ,van der Geest RJ,et al. Infarct tissue heterogeneity assessed with contrast-enhanced  
366 MRI predicts spontaneous ventricular arrhythmia in patients with ischemic cardiomyopathy and  
367 implantable cardioverter-defibrillator. *Circ Cardiovasc Imaging.* 2009;2:183–190.
- 368 20. Nazarian S,Bluemke DA,Lardo AC, et al. Magnetic resonance assessment of the substrate for inducible  
369 ventricular tachycardia in nonischemic cardiomyopathy. *Circulation.* 2005;112:2821–2825.
- 370 21. Perin EC,Silva GV,Sarmiento-Leite R, et al. Assessing myocardial viability and infarct transmural  
371 left ventricular electromechanical mapping in patients with stable coronary artery disease: validation by  
372 delayed-enhancement magnetic resonance imaging. *Circulation.* 2002;106:957–961.
- 373 22. Codreanu A,Odille F,Aliot E, et al. Electroanatomic characterization of post-infarct scars comparison with  
374 3-dimensional myocardial scar reconstruction based on magnetic resonance imaging. *J Am Coll Cardiol.*  
375 2008;52:839–842.
- 376 23. Esposito A,Palmisano A,Antunes S,et al. Cardiac CT With Delayed Enhancement in the Characterization  
377 of Ventricular Tachycardia Structural Substrate: Relationship Between CT-Segmented Scar and  
378 Electro-Anatomic Mapping. *JACC Cardiovasc Imaging.*2016;9:822-832.

**Table 1. Patient Characteristics (N=9)**

Pt No	Age	Gender	Scar location	EF	Procedure No	HT	DM	DL	smoking	ICD	beta-blocker	Amiodarone
1	59	M	Inferior, lateral	25	3	y	n	y	y	y	y	y
2	29	M	Anterior, lateral	28	3	n	n	n	n	y	y	n
3	62	M	Anterior, septal	30	1	y	n	y	cessation	y	y	y
4	75	M	Inferior, septal	40	4	y	n	y	y	y	y	y
5	47	F	Anterior, septal	31	1	n	n	n	y	y	y	n
6	48	M	Anterior, septal	30	2	n	n	y	y	y	y	y
7	71	M	Inferior, lateral	40	4	y	y	y	cessation	y	y	y
8	68	M	Inferior, septal	45	1	y	n	y	y	y	y	n
9	72	F	Inferior	36	1	n	n	y	y	y	y	y

DL,Dyslipidemia; DM,diabetes mellitus; EF,ejection fraction; F,female; HT,hypertension; ICD,implantable cardioverter defibrillator; M,male

382 **Table 2. CT-channel**

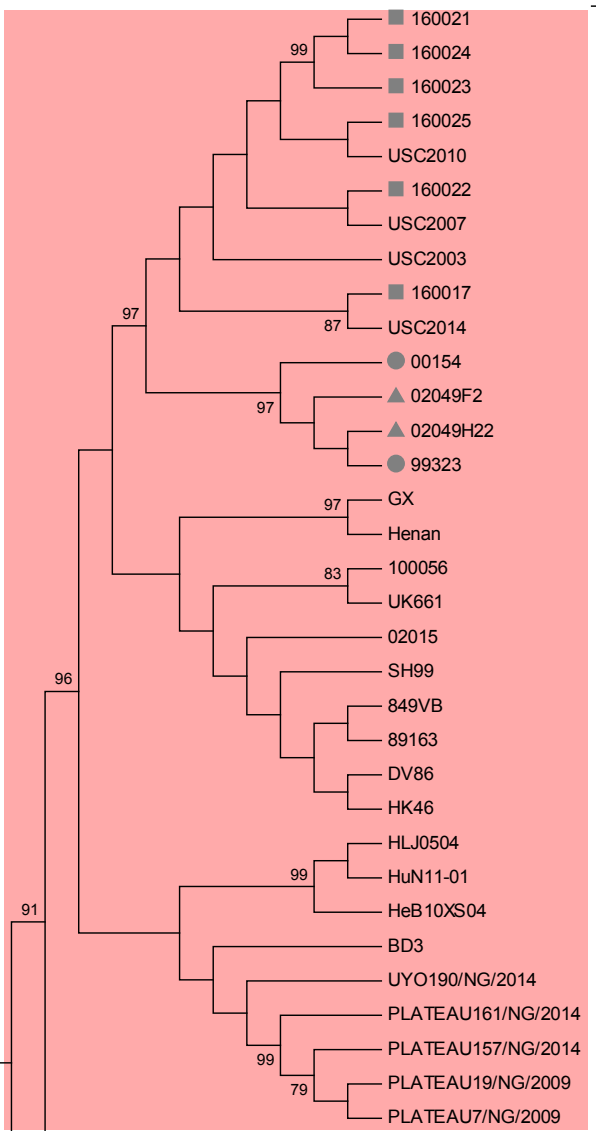
Pt No.	Total scar area, cm <sup>2</sup>	Dense scar area ,cm <sup>2</sup>	Number of CT-channel	Length, mm	Width, mm	Area, cm <sup>2</sup>	WT (channel center) ,mm	WT (channel edge) ,mm	Channel parallel to the MA
1	121.81	44.71	4	37.8[24.0-58.4]	11.9[10.0-17.5]	1.93[1.63-4.43]	2.4[2.2-3.4]	1.9[1.5-2.3]	3[75.0%]
2	118.92	13.26	7	20.7[17.6-26.1]	7.9[7.3-11.5]	1.03[0.88-1.74]	3.5[2.3-3.7]	2.9[2.1-3.1]	4[57.1%]
3	110.1	60.8	7	38.8[31.4-62.0]	14.0[9.2-32.0]	1.46[1.23-12.0]	2.3[1.9-3.5]	1.3[0.9-1.7]	4[57.1%]
4	46.4	20.2	3	17.7[9.9-36.8]	8.6[7.9-9.0]	1.59[0.90-1.92]	2.1[1.0-2.5]	0.8[0.6-0.9]	2[66.7%]
5	47.7	17.1	4	15.0[11.0-21.7]	5.1[3.4-9.8]	0.90[0.54-1.34]	2.3[2.0-2.7]	1.4[0.7-1.6]	4[100%]
6	85.1	24.8	7	33.2[30.0-44.9]	16.5[10.9-19.9]	1.75[1.55-3.58]	3.0[2.1-4.6]	1.3[0.9-1.7]	2[28.6%]
7	86.4	51.9	1	52.5	18.1	3.79	2.1[2.1-2.1]	0.7[0.7-0.7]	1[100%]
8	45	8	5	18.7[15.6-22.6]	7.2[6.4-16.8]	1.29[1.11-1.75]	2.8[2.3-3.5]	2.0[1.9-2.4]	3[60.0%]
9	54.9	36.3	3	36.8[33.2-41.1]	7.7[7.0-44.6]	1.76[1.11-2.78]	1.7[1.2-2.1]	0.6[0.6-0.9]	2[66.7%]
Median	85.1[47.1-114.5]	24.8[15.2-48.3]	4[3-7]	30.0[18.5-40.2]	10.9[7.2-15.9]	1.55[1.05-2.28]	2.4[2.1-3.5]	1.6[0.9-2.2]	24/41[58.5%]

383

384 CT,computed tomography; MA,mitral annulus; WT,wall thickness

385

# A- Segment A



vvIBDV (g3)

Classical IBDV (g1)  
US antigenic variants (g2)

Cell culture adapted and vaccine strains

Divergent IBDV (g4)

Italian IBDV (g6)

Australian IBDV (g7)

Serotype 2 IBDV

# B- Segment B

